

Article

# Molecular Cloning and Expression Analysis of COX II from *Sitophilus zeamais*, a Potential Action Site of AITC

Changliang Hou<sup>1</sup>, Jingbo Wang<sup>1</sup>, Hua Wu<sup>1,2,\*</sup>, Jiayu Liu<sup>1</sup>, Zhiqing Ma<sup>1,2</sup>, Juntao Feng<sup>1,2</sup> and Xing Zhang<sup>1,2</sup>

<sup>1</sup> Research and Development Centre of Biorational Pesticides, Northwest Agriculture and Forestry University, Yangling 712100, China; hou2014050242@nwsuaf.edu.cn (C.H.); wangjingbo@nwsuaf.edu.cn (J.W.); ljj1691005353@icloud.com (J.L.); zhiqingma@nwsuaf.edu.cn (Z.M.); jtfeng@126.com (J.F.); zhxing1952@gmail.com (X.Z.)

<sup>2</sup> Research Center of Biopesticide Technology and Engineering, Yangling 712100, China

\* Correspondence: wgf20102010@nwsuaf.edu.cn; Tel./Fax: +86-29-8709-2122

**Abstract:** COX II containing a dual core CuA active site is one of the three core subunits of mitochondrial Cco, which plays a significant role in the physiological process. In this report, the full-length cDNA of COX II gene was cloned from *Sitophilus zeamais*, which had an ORF of 684 bp encoding 227 amino acids residues. The predicted COX II protein had a molecular mass of 26.2 kDa with pI value of 6.37, and multiple sequence alignment and phylogenetic analysis indicated that *Sitophilus zeamais* COX II had high sequence identity 78.51% with the COX II of other insect species, especially similarity to *sitophilus oryzae*. This gene was subcloned into the prokaryotic expression vector pET-32a, and induced by IPTG in *E.coli* Transetta (DE3) expression system. Finally the COX II with 6-His tag was purified using affinity chromatography with Ni<sup>2+</sup>-NTA agarose. WB showed the recombinant COX II was about 44 kD, and the concentration of fusion protein was 50µg/mL. UV-spectrophotometer and infrared spectrometer analysis showed that recombinant COX II could catalyze the oxidation of substrate Cyt<sub>c</sub>, and influenced by AITC. It was found that AITC could form a hydrophobic region with COX II protein via molecular docking, besides, a sulfur atom of AITC structure could form a length of 2.9 Å hydrogen bond with Leu-31. These results will provide valuable information for elucidating the role of COX II in *Sitophilus zeamais* responses to AITC, meanwhile, it will helpful to carry out a point mutation in AITC binding sites for the future research.

**Keywords:** *Sitophilus zeamais*; COX II; Soluble proteins; Enzyme activity; AITC

## 1. Introduction

*Sitophilus zeamais* is one of the major pests of stored products in the tropics and subtropics [1-2]. For a long time, management of the stored product pests has relied on synthetic insecticides and fumigants, such as metal phosphide [3-4], methyl bromide [5] and sulfuryl fluoride [6]. However, the use of fumigants has led to serious problems like 3R (resistance, resurgence, and residue) *ect* [7-9], therefore, it is urgent to find a new type of alternative fumigants to prevent and control *Sitophilus zeamais*.

In recent years, it has been proved that AITC released from glucosinolates in Brassicaceous residues have a strong fumigation activity against stored grain pests [10-12], while the mechanisms of AITC on target organisms are still relatively scarce. Our research group found that AITC had a significantly effect on mitochondrial respiratory chain Cco of *Sitophilus zeamais* *in vivo* and *in vitro* [13]. ROS produced by AITC could further damage the mitochondrial membrane potential, leading to the defect of mitochondrial function (Figure 1). Due to the above similar pathophysiology alterations and destructive structure of mitochondria, AITC and phosphine were proposed to act by similar mechanisms [14].

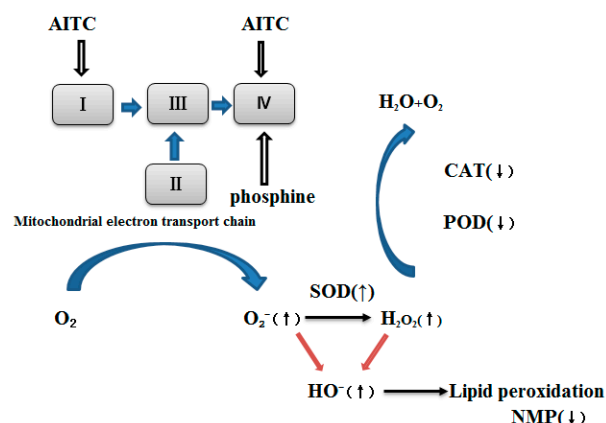


Figure 1. Proposed scheme for AITC-induced mitochondrial dysfunction with phosphine as the positive control. Arrows in parentheses represent for increase (up) or decrease (down) in activity or amount induced by AITC and phosphine fumigation

It was generally known that Cco was the terminal metal membrane protein in the electron transport chain of the eukaryotic mitochondrial inner membrane and the aerobic bacteria cell membrane electron transfer chain, and played a significant role in the physiological process [15-17]. Cco was a complex enzyme consisting of 13 different subunits in mammalian cells [18-19], and only the core subunits I–III were encoded by the mitochondrial genome [20]. These subunits were highly conserved among different organisms and were the key components of bacterial oxidases as well. Subunit I had two heme a moieties (a and a<sub>3</sub>) and a copper ion (Cu<sub>B</sub>), and the latter two formed the binuclear center catalyzing oxygen reduction. Subunit II carried two copper ions in its Cu<sub>A</sub> center, a hydrophilic domain oriented to the intermembrane space. During the stepwise reduction of Cox, cytochrome c docks to this domain and transfers one electron at a time to the Cu<sub>A</sub> center. Much work had been done concerning Cco but a little about cloning and expression of COX II from *Sitophilus zeamais* [21-24].

In this study, the COX II from *Sitophilus zeamais* was cloned, and the recombinant enzyme was expressed in *E.coli* under different IPTG concentration, time and temperature. In addition, we analyzed the sequence and examined the activity of the enzyme. This work could provide the basis information for the study of mechanism of AITC against *Sitophilus zeamais*.

## 2. Results

### 2.1 Cloning and Sequence Analysis

A 3' cDNA fragment of 532 bp and a 5' cDNA fragment of 305 bp were amplified by 3' and 5' RACE using the special primers (Table 1). The full-length cDNA of 684 bp was then obtained by RT-PCR based on the cDNA sequences of the 3' and 5' RACE fragments. The cDNA sequence of COX II had an ORF of 684 bp encoding 227 amino acid residues (Figure 2) with a molecular weight of 26.2 kDa, and an isoelectric point of 6.37.

Multiple alignments of COX II deduced amino acid sequence with other insect species in NCBI database was shown below (Figure 3). COX II exhibited a high degree of 78.51% identity conservation with other insects. To investigate the evolutionary relationships of the COX II from *Sitophilus zeamais* with other insect COX II, a phylogenetic tree was constructed from the deduced amino acid sequences from 14 species of COX II (Figure 4). The analysis showed that the *Sitophilus zeamais* COX II was located on the same branch with *Sitophilus oryzae*, however, *Sitophilus zeamais* COX II had a distant phylogenetic relationships with *Vespa bicolor*, *Bombyx mori* and *Drosophila melanogaster*. The relationships displayed in the phylogenetic tree corresponded to their taxonomic classifications.

```

1   ATATCAACATGAAAACTCTTTTCTTCAAGATAGAGCCTCACCTTTAATAGAACATCTT
   M S T W K T L F L Q D S A S P L M E H L
61  ACATTATTTTCATGACCATACTATTTTAATCTTAATTTTAATTACAATTTTAGTTAGACAA
   T L F H D H T I L I L I L I L I T I L V S Q
121 ATACTATTAAGAATATTATTAATAAACTCTCACACCGATTTTACTTGAAGTCAATTA
   M L L S M L L N K L S H R F L L E G Q L
181 ATTGAAACTATTTGAACTATTCTACCTGCTATTATTCTTATTTTAATTCCTTACCCTCA
   I E T I W T I L P A I I L I L I A L P S
241 CTTCGATTATTATACATTCTAGACGAAATTAATAACCCTTCTATTACTATTAATAATTATC
   L R L L Y I L D E I N N P S I T I K I I
301 GGACATCAATGATATTGATCATATGAATATTCTGATTATAAAAAATATTGAATTTGATTC
   G H Q W Y W S Y E Y S D Y K N I E F D S
361 TATATAATTCCTACCAAGAAGACTTAACTCTTTTAATTTTCGTCCTTAGAAGTAGATAAT
   Y M I P T K E L N S F N F R L L E V D N
421 CGAACTCCTTTTCTTATAAACTCAAATTCGACTCTTAGTTACGTCTGCAGATGTAATT
   R T P F P Y K T Q I R L L V T S A D V I
   CuA binding site [ion binding site]
481 CATTCTGGACAGTACCAAGTATAGGAATAAAATGATAGAACCCAGGACGCTTAAAT
   H S W T V P S M G I K I D S T P G R L N
   CuA binding site [ion binding site]
541 CAAGCCAATTTAATTGCTAATCGTTCAAGAATCTTTTTGGCCAATGTTCTGAAATTTGC
   Q A N L I A N R S S I F F G Q C S E I C
   CuA binding site [ion binding site]
601 GGAGCAAACCATAGATTTATACCTATCATTTTAGAAAAGAATTAACCCAATTTATTTTAA
   G A N H S F M P I I L E S I K P N L F L
661 AACTGAATTATTTCCAAAACITAA
   N W I I S K T *

```

**Figure 2.** Nucleotide and amino acid sequence of *Sitophilus zeamais*. CuA binding site [ion binding site] containing 6 conserved feature residue pattern: H C E C H M were indicated by grey color. The start codon and the stop codon were represented with an asterisk (\*)

Bombyx_mori	.....MATWSNINICNGASPLMEQIIFPHDHTLITITITLIVSYLMISLFPNKYINRFLLEGQMELEIWTIMFAFT	72
Vespa_bicolor	.....MCTRLNFYICDNTFNMNOLIMFHYSMIMLITLISLISYMFIFLIMNKITNRFMTNEHFEIITWITIMFLT	72
Tribolium_castaneum	.....MATWKLMLMDSASPLMEQLSEFHDHTLITITITLIVGOMMAGLFVNRKLTFRFLLEGQMELEIWTIVLPAIT	72
Sitophilus_oryzae	.....MSTWKTILFDCDSASPLMEHLITLPHDHTLITITITLIVSOMLLSMLLNKLSHRFLLEGQMELEIWTIIPAIT	72
Sitophilus_granarius	.....MSTWKNLFLDCDSASPLMEHLMFPHDHTMLITITITIMVSOMLLSMLPNKLSHRFLLEGQMELEIWTIIPAIL	72
Rhynchophorus_ferrugineus	MKLTFLFLEISTWKTMLMDCDSASPLMEQLMSEFHDHALLITITITLIVSOVLLNFRNKFSTRFLLEDQLEIWTIIPAIL	80
Sitophilus_zeamais	.....MSTWKTILFDCDSASPLMEHLITLPHDHTLITITITLIVSOMLLSMLLNKLSHRFLLEGQMELEIWTIIPAIT	72
Consensus	tw q p m fhd l it nk r ie iwt p	
Bombyx_mori	LIFLTAIPSLRLLYLLDEINNPSTITKIGHQWYWSYSEYDFDNIEFDSYMIPTKELNSFNRLLEVDNRTTPFYKTCIRI	152
Vespa_bicolor	LIMTAIPSLKILYMTSEFFSPTLITRAIGHQWYWSYVELSDYKRNIEFDSYMIPTKKTNQSQFRLLDVDNRLIIPFDTEIRI	152
Tribolium_castaneum	LIFLTAIPSLRLLYLLDEINNPSTITKIGHQWYWSYSEYDFDNIEFDSYMIPTKELNSFNRLLEVDNRTTPFLSICIRI	152
Sitophilus_oryzae	LIFLTAIPSLRLLYLLDEINNPSTITKIGHQWYWSYSEYDFDNIEFDSYMIPTKELNSFNRLLEVDNRTTPFYKTCIRI	152
Sitophilus_granarius	LIFLTAIPSLRLLYLLDEINNPSTITKIGHQWYWSYSEYDFDNIEFDSYMIPTKELNSFNRLLEVDNRTTPFYKTCIRI	152
Rhynchophorus_ferrugineus	LIFLTAIPSLRLLYLLDEINNPSTISVRAIGHQWYWSYSEYDFDNIEFDSYMIPTKELNSFNRLLEVDNRLIIPFETCIRI	160
Sitophilus_zeamais	LIFLTAIPSLRLLYLLDEINNPSTITKIGHQWYWSYSEYDFDNIEFDSYMIPTKELNSFNRLLEVDNRTTPFYKTCIRI	152
Consensus	l ia psl y e p k ighqwywsye d ni fdsymip frll vdnr p ir	
Bombyx_mori	MITATDVIHSWTHPSLGVKVDANPGRINQTFFFINRPGTFEGQCSEICGNHSMFPIVIESISIKNFILWLNNSYS	227
Vespa_bicolor	LITSDVIHSWTHPSLGVKVDANPGRINQTFFFINRPGTFEGQCSEICGNHSMFPIVVESTSLSFIKMNINNM.	226
Tribolium_castaneum	LVSADVHSWTHPSLGVKVDANPGRINQTFSTRSSLMYGCSEICGNHSMFPIVAESTIAPSYFIKWLISKMI	227
Sitophilus_oryzae	LVTSADVHSWTHPSMGIKDSTPGRINQANLIANRSSIFEGQCSEICGNHSMFPIVLESITKENFILWNLISKT	227
Sitophilus_granarius	LVTSADVHSWTHPSMSTKDDGTPGRINQANLIANRSSIFEGQCSEICGNHSMFPIVLESITKENFILWNLISKT	227
Rhynchophorus_ferrugineus	LVSLLDVIHSWTHPSLGVKDDGAPGRINQVGLIINRPGTFEGQCSEICGNHSMFPIVIESISPKYFLRWLISQ.	234
Sitophilus_zeamais	LVTSADVHSWTHPSMGIKDSTPGRINQANLIANRSSIFEGQCSEICGNHSMFPIVLESITKENFILWNLISKT	227
Consensus	dvihswt p k d pgr nq r gqcseicg nhsmfpi es f w	

**Figure 3.** Multiple alignments of the amino acid sequence with other known COX II. The multiple alignment was analyzed on DNAMAN 8.0. Dark blue: identity =100%; red: 75%≤identity <100%; light blue: 50%≤identity ≤75%. The absent amino acids in the alignment were indicated by dots (.), identical residues are indicated with lowercase. The GenBank accession numbers of the COX II were as follows:*Bombyx mor* (AAK85720.1), *Vespa bicolor* (AIE42617.1), *Tribolium castaneum* (AIM19612.1), *Sitophilus oryzae* (ANW06522.1), *Rhynchophorus ferrugineus* (YP-009183673.1), *Sitophilus granarius* (JN163959.1), respectively.

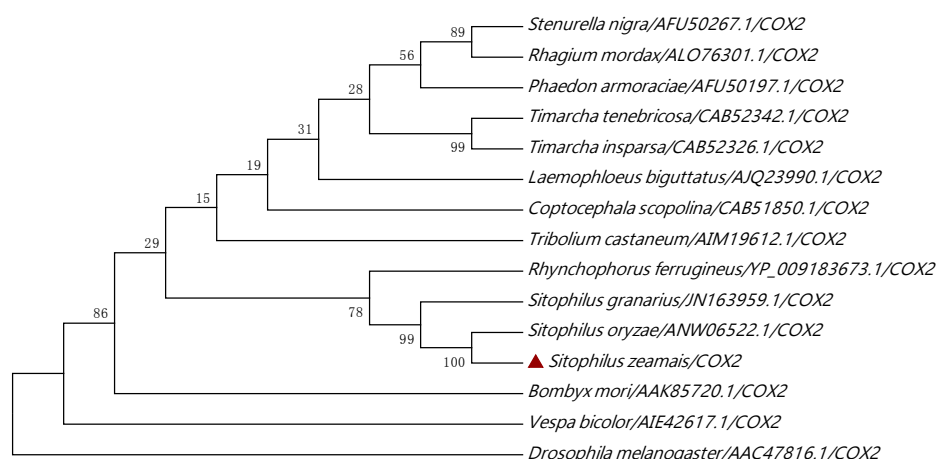


**Figure 4.** Phylogenetic analysis of the amino acid sequences of *Sitophilus zeamais* COX II. The Neighbor-Joining phylogenetic trees were constructed using the bootstrap method on MEGA 5.1 and the number of Bootstrap replications was 1000. The protein sequences used in these trees were as follows: *Timarcha tenebricosa* (CAB52342.1), *Timarcha insparsa* (CAB52326.1), *Rhagium mordax* (ALO76301.1), *Drosophila melanogaster* (AAC47816.1), *Bombyx mori* (AAK85720.1), *Vespa bicolor* (AIE42617.1), *Tribolium castaneum* (AIM19612.1), *Rhynchophorus ferrugineus* (YP\_009183673.1), *Phaedon armoraciae* (AFU50197.1), *Coptocephala scopolina* (CAB51850.1), *Laemophloeus biguttatus* (AJQ23990.1).

## 2.2 Effect of temperature, IPTG concentration and processing time on solubility of COX II

To investigate the effect of temperature on the solubility of recombinant COX II protein, N-terminal Trx/6-His/S tagged COX II protein was over-expressed in *E. coli* Transetta (DE3) at 37°C, 25°C and 16°C, respectively. It was found that the majority of the recombinant protein was insoluble at 37°C and 25°C after sonication (Figure 5A). Compared with the protein generated at 37°C and 25°C, when the recombinant cells overexpressed at 16°C produced a higher percentage of soluble protein. The recombinant protein was further determined by WB analysis (Figure 5B). In general, the soluble protein yield corresponded negatively to the elevating temperature.

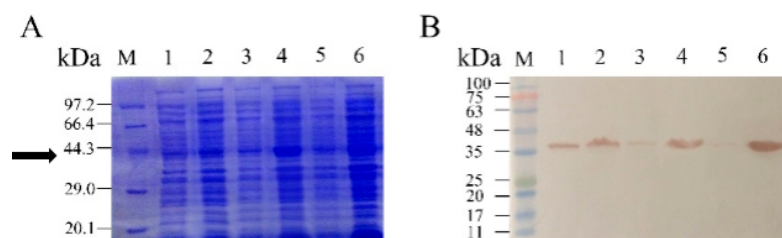


**Figure 5.** Analysis of the effect of temperature on the solubility of fusion COX II protein. (A) SDS-PAGE was carried out by a 12 % polyacrylamide gel. (B) Western blotting analysis of fusion COX II using anti-His tag antibody. The fusion COX II was expressed in *E. coli* Transetta (DE3) at 16°C (lanes 1 and 2), 25°C (lanes 3 and 4), 37°C (lane 5 and 6). The soluble fractions are shown in lanes 1, 3 and 5, respectively. Lane M, molecular mass marker proteins. The arrow indicates the expected size of fusion COX II protein.

Attempts had also been conducted to increase the fraction of soluble protein in *E. coli* by adding IPTG at different levels (Figure 6). Higher IPTG was found to have negative influence on the rate of cell growth, which suppressed the *E. coli* Transetta (DE3) cell growth. The solubility of COX II content reached its highest in the presence of 1mM IPTG.

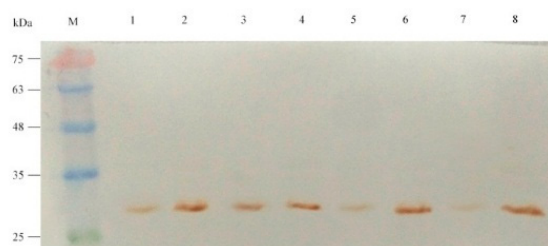


**Figure 6.** Western blot analysis of the effect of IPTG concentration on the solubility of recombinant fusion COX II protein. The fusion COX II was expressed in *E. coli* Transetta (DE3) under 0.5 mM (lanes 1 and 2), 1.0 mM (lanes 3 and 4), 1.5 mM (lanes 5 and 6), 2.0 mM (lanes 7 and 8). The soluble fractions are shown in lanes 1, 3, 5 and 7 respectively. Lane M, molecular mass marker proteins.

Different processing time was also carried out to investigate its influence on the solubility of COX II. The results showed that with the extension of culture time, the protein content was increasing at the range from 6 to 24 h, (Figure 7), however, the soluble content of protein was decreased with the prolongation of the culture time after cultured 24h. In a word, it was concluded that the solubility of COX II was expressed highly in *E. coli* Transetta (DE3) at condition of 1 mM IPTG, 16°C, 24 h, and 200 rpm.

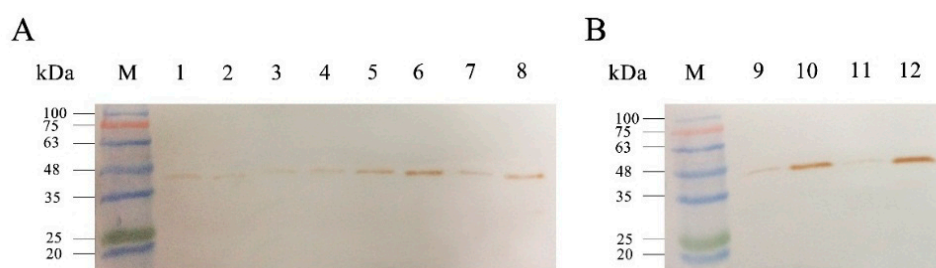


**Figure 7.** Western blot analysis of the effect on the solubility of recombinant COX II protein in the different treatment time. The fusion COX II was expressed in *E. coli* Transetta (DE3) with 6 h (lanes 1 and 2), 12 h (lanes 3 and 4), 24 h (lanes 5 and 6), 36 h (lanes 7 and 8), 48 h (lanes 9 and 10), and 60 h (lanes 11 and 12). The soluble fractions were shown in lanes 1, 3, 5, 7, 9 and 11 respectively. Lane M, molecular mass marker proteins.

### 2.3 Purification of COX II protein and Western Blot Assay

The COX II protein was purified as described in “materials and methods” section, and the purified recombinant protein (eluted at 200 mM concentration of imidazole) presented a single band on SDS-PAGE (Figure 8A). The Mw of purified protein band was about 44 kDa larger than the predicted 26 kDa due to the N-terminal Trx/6-His/S-tagged. The Trx-free recombinant COX II protein was generated by enterokinase digestion and migrated as a single band estimated as 26 kDa (Figure 8 A) which corresponded to the size of predicted Mw. The WB signal was detected for recombinant enzyme produced from pET32a vectors (Figure.8 B). The concentration of purified COX II was 50 mg•L<sup>-1</sup> based on Bradford assay.

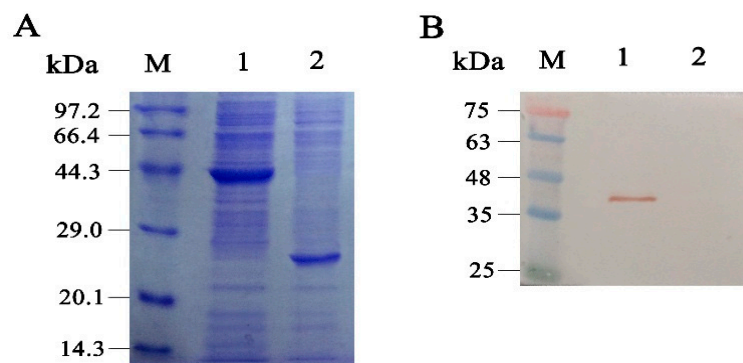


**Figure 8.** SDS-PAGE and Western blot analysis of purified recombinant COX II. (A) The samples were separated on 12% gels; and (B) Western blot analysis of recombinant COX II using anti-His tag antibody. Lane M: protein molecular standard, Lane 1: purified Trx/6×His/S-tag/COX II from pET32a, Lane 2:Trx-free COX II protein digested by enterokinase.

## 2.4 Enzymatic activity of the COX II

The purified tag-free protein was characterized by using the UV-visible. Under certain concentration of substrate Cytc, the absorption peak of Cytc at 520nm and 550nm decreased gradually with the increase of enzyme concentration. Besides, by adding different concentrations of AITC to the substrate Cytc, there was no change at the maximum absorption peak, while adding purified COX II to the solution containing AITC and reduced Cytc, the absorption peak was still unchanged. So, the fusion COX II protein could have an activity towards Cytc and affected by AITC according to the above treatments of three groups (Figure 9). In order to confirm whether AITC combination with recombinant COX II, the reaction system of both them was detected by infrared spectrometer. while hypochromic shift was observed at 3400nm, which indicated that AITC is combined with the end of COX II (Figure 10)

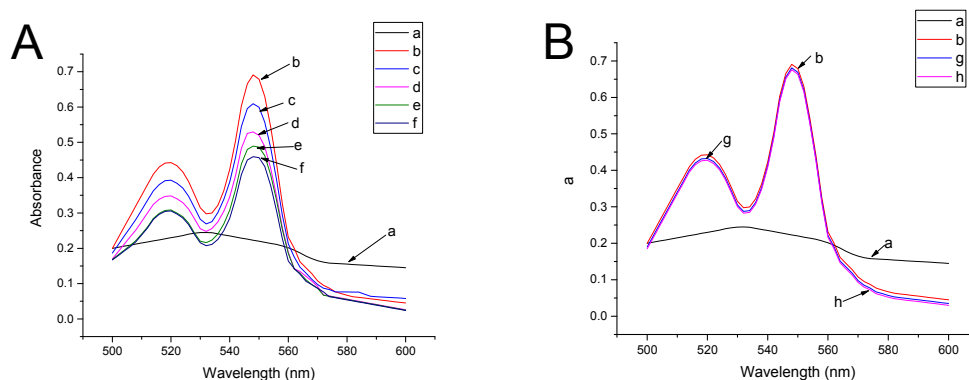


**Figure 9.** Measuring the activity of *Sitophilus zeamais* COX II. **a:** Oxidized Cyt c; **b:** Reduced Cyt c; **c:** Reduced Cyt c C+2µL purified COX II; **d:** Reduced Cyt c C+4µL purified COX II; **e:** Reduced Cyt c C+8µL purified COX II; **f:** Reduced Cyt c C+16µL purified COX II; **g:** Reduced Cyt c C+2µL AITC; **h:** Reduced Cyt c C+2µL AITC+4µL purified COX II

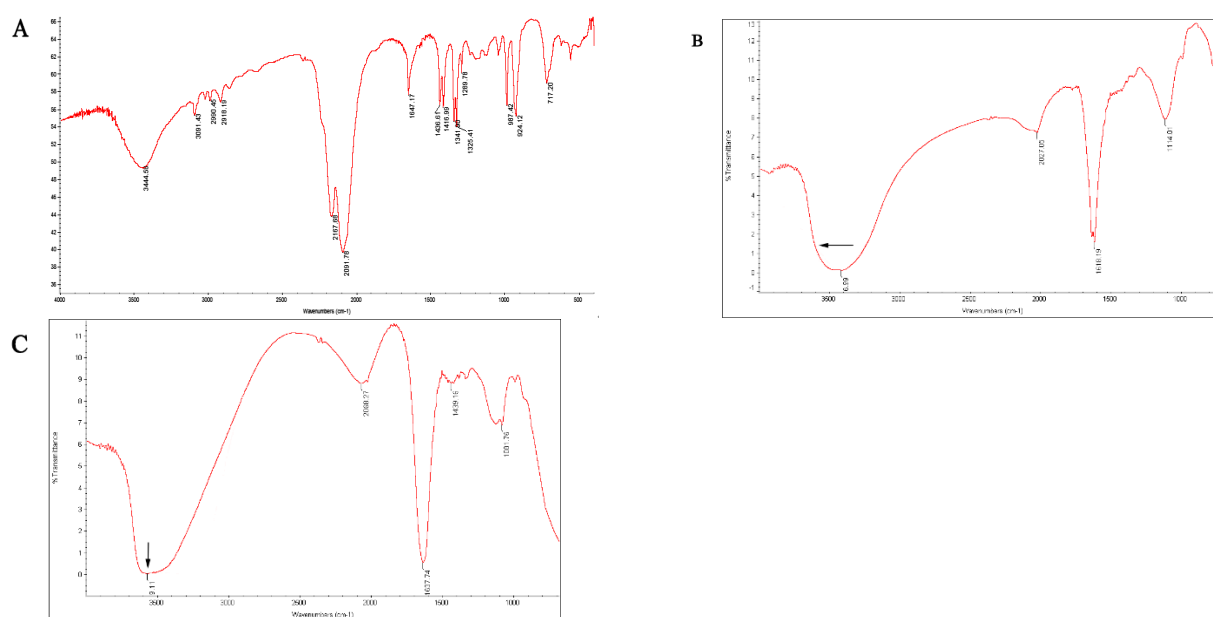


**Figure 10.** Infrared spectrometer scan map of samples. (A) Absorption peak of AITC. (B) absorption peak of purified COX II. (C) absorption peak of AITC and purified COX II. Absorption peak at 3400 wavenumber of N-terminal or C-terminal of the purified COX II was shifted to 3600 wavenumber after adding AITC.

## 2.5 Homology modeling and molecular docking

To further understand the action sites of AITC effected on COX II. The specific location of AITC interaction with Cco was simulated by molecular docking using the Vina 1.1.2 Autodock and Discovery Studio (DS) (Accelrys, USA) software at the molecular level. Analysis showed that the propylene group of AITC was located in a

hydrophobic cavity formed by the amino acid residues Ile-34, Pro-69, Ile-72, Leu-73 and Ile-76, forming a strong hydrophobic interaction (Figure 11).

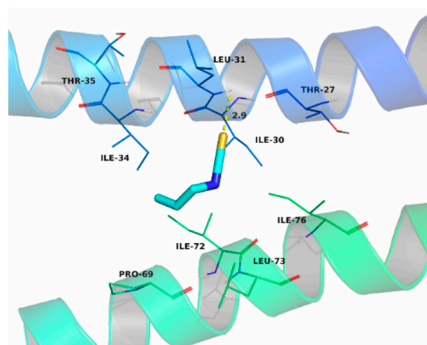


**Figure 11.** Molecular docking of AITC effect on the active site of *Sitophilus zeamais* COX II by using Vina 1.1.2 Autodock and Discovery Studio software at the molecular lever.

### 3. Discussion

In recent years, a number of mechanisms have been proposed for the activities of AITC [25-33], such as microtubule, proteasome, nucleus, mitochondria, ABC transporters and TPR channel. However, identifying the molecular targets is a first step to make sure the molecular mechanisms of AITC. Mitochondria of insect had been proved to be the main AITC's target. [12, 34]. Our research group found that AITC had a significantly effect on mitochondrial respiratory chain Cco of *Sitophilus zeamais* *in vivo* and *in vitro* [13]. ROS induced by AITC could further damage the mitochondrial membrane potential, leading to the defect of mitochondrial function. Basing on the similar pathophysiology alterations and destructive structure of mitochondria, AITC and phosphine are proposed to act by similar mechanisms [14]. So, Cco target of AITC was proposed.

There is a great interest in Cco due to its role in the respiratory chain of mitochondria including transfer of electrons from Cyt c to O<sub>2</sub> and function coupled with proton pump [35-37]. To investigate the function and activity of COX II, it is necessary to obtain the pure enzyme by separation from tissues, or expression and purification from a heterogeneous system. In this study, COX II gene from the *Sitophilus zeamais* was cloned, sequenced and analyzed. COX II ORF contain A+T=72.7%, G+C=27.3%, consistent with previously reported [38]. Bio-informatic and phylogenetic analysis clearly suggested that COX II shared high sequence similarity with COX II genes of other insects, especially similarity to *sitophilus oryzae*. The reason for the results was that the COX II subunit was highly conserved in the long process of biological evolution. Multiple alignment analysis and phylogenetic trees also showed that varied of COX II identity and homology had a certain degree of difference as well as the relative conservation. This was able to exercise its unique biological function among different species.

There are two different coding systems for the mitochondrial genome and nuclear gene coding. According to the invariance of the sequence of the target protein sequence, the obtained COX II subunit gene was modified, synthesized and then expressed. Different expression vectors (Peasy blunt E1, pET28a, pET30a, pET32a, pET42a) were used to express COX II fusion protein. However, only pET32a-COX II could be expressed recombinant protein in the *E.coli* Transetta(DE3) and be detected by the SDS-PAGE and WB. After removal of fusion tag with enterokinase, the monomeric form of COX II could not be visualized by WB because of the lack of anti-COX II antibodies.

Overexpression of protein in heterologous systems often results in the formation of inclusion bodies [39]. In the *E. coli* expression system, the formation of inclusion bodies can be formed owing to the high growth rates of cell lead to the protein unfolded to form the correct conformation [40]. Therefore, improving solubility is a major goal in studying protein production processes. Recently, the use of low growth temperatures to increase soluble protein yields has been reported [41-42]. In present study, most of the COX II protein expressed in *E.coli* was as inclusion bodies. Therefore, various strategies have been designed to overcome this drawback. When expressed at 37°C, a considerable amount of the total protein in *E. coli* BL21 (DE3) was obtained, however only a little soluble protein was detected. Finally, considerable soluble protein was obtained when expressed at 16°C, accompanied by a reduced total protein yield. The results suggested that the conformational quality of COX II protein is significantly

influenced by temperature. When grown at low temperature, COX II proteins with the slow rates growth in *E. coli* cell have enough time to fold in the correct conformation [43].

After removal of fusion tag with enterokinase, UV-visible was used to characterize purified COX II active site. Although the *E. coli* system was a very convenient expression system to obtain purified recombinant protein *in vitro*, it was usually unsuitable to be used for the expression of the recombinant protein from most eukaryotes, such as insects, plants, and so on, because of highly divergent codon usage and protein misfolding [43, 44]. The Cyt<sub>c</sub> could not be oxidized into a fully oxidized state, the reasons are as follows: (1) the activity of COX II needed the interaction of Cco subunits, for example, subunit III played an important role in the integrity of the structure and function of the enzymes [45-49]; (2) purified protein concentration was too low to maintain the integrity structure of biological macromolecules, resulting in changes in the spatial structure of the copper center in the enzyme; (3) as the reaction system was carried out, the pH of the buffer was changed leading to the change of the structure of the enzyme, which affected the activity of the enzyme [50].

The absorption peak of Cyt<sub>c</sub> at 520 nm and 550 nm decreased gradually with the increase of enzyme concentration. While adding AITC or "AITC + purified COX II" into Cyt<sub>c</sub> system, the absorption peak did not change significantly. To explain this phenomenon, a molecular docking and analysis was conducted. The results demonstrated that the propylene group of AITC was located in a hydrophobic cavity formed by the amino acid residues Ile-34, Pro-69, Ile-72, Leu-73 and Ile-76, forming a strong hydrophobic interaction. Moreover, the sulfur atom in AITC with amino acid residues Leu-31 growth for the interaction of a hydrogen bond 2.9 Å. It might be predicted that AITC have the strong inhibitory action to the COX II activity.

## 4. Materials and methods

### 4.1. Insects

*Sitophilus zeamais* cultured in the laboratory were provided by the Northwest Agriculture and Forestry University, Shannxi Province in China. Feeding wheat was placed in an oven (80°C) for 2 hours, and then adjusted the moisture content to 14%, divided and inoculating at 28°C±1°C, 75%±5% relative humidity, a photoperiod of 16:12(Light: Dark), 25±1°C for 7 days. *Sitophilus zeamais* strain was reared for generations and selected the same size of insects for the experiment.

### 4.2. Chemicals and Plasmids

*EcoRI*, *XhoI*, prime STAR Max Premix, *E. coli* DH5 $\alpha$ , T4 DNA ligase and protein marker were purchased from Takara (Dalian, China). *E. coli* Transetta (DE3) was obtained from TransGen Biotech (Beijing, China). Horseradish peroxidase (HRP)-labeled Anti-His Tag Mouse Monoclonal Antibody and HiFiScript gDNA Removal cDNA Synthesis Kit were ordered from Kang bio-technology of the century (Beijing, China). The E.Z.N.A Plasmid Mini kit was provided by Omega (Guangzhou, China). Cytochrome c from bovine heart was purchased from Sigma (USA), and pET32a were used for protein expression. All other chemicals were analytical grade and obtained from Shanghai Sangon (Shanghai, China).

### 4.3. RNA extraction and cDNA synthesis for Molecular Cloning

The total RNA from *Sitophilus zeamais* was extracted by using the modified CTAB method [51]. The quality and concentration of extracted RNA was examined by 1% agarose gel electrophoresis and SpectraMax Plus<sup>384</sup>. The total RNA was digested with DNase I to remove the genomic DNA and for cDNA synthesis. 5'RACE and 3'RACE-Ready cDNA were synthesized from 1  $\mu$ g of total RNA using the SMART<sup>TM</sup> RACE cDNA Amplification Kit (Clontech, Dalian, China) as described by the manufacturer, respectively. The products were stored at -20°C for future use.

### 4.4. Molecular Cloning of COX II cDNA by 3' and 5'RACE

The primers used for 3' and 5'RACE amplification were designed (Table 1) according to the known partial sequence of *Sitophilus zeamais* in the NCBI database using the Primer Premier 5(PP5). 3'-RACE PCR was conducted using C2-1F1 and 10 $\times$  Nested universal Primer A (NUP) as the primer pair for the PCR reaction. For 5'RACE, PCR was carried out using C2-1R1 and 10 $\times$ Universal Primer a Mix (UPM) as the primer pair for PCR amplification. For both 3' and 5'RACE, the PCR reaction conditions were: 95°C for 3 min, followed by 32 cycles of 30 s at 95°C, 45 s at 55°C and 1 min at 72°C, and then final extension at 72°C for 5 min. The PCR products were separated on a 1% agarose gel electrophoresis and purified using Gel Extraction Kit (Omega, Guangzhou, China). The purified fragments were ligated into the pMD-19T vector (Takara, Dalian, China) and positive clones were



sequenced (Sangon, Shanghai, China). Based on the obtained sequences of the 3' and 5'RACE, the splicing full-length of COX II gene was amplified with specific primers C2-qF and C2-qR.

**Table 1.** List of primers used in this study.

Name	Sequence (5'-3')	Primer used
C2-1R1	ATTAAATTGGCTTGATTTAGACGACCT	5'RACE
5'-RACE CDS Primer	(T)25V N	5'RACE
SMART II A Oligonucleotide	AAGCAGTGGTATCAACGCAGAGTACATGGG	5'RACE
C2-1F1	CACCTTACCTTATCCATGATCACACT	3'RACE
3'-RACE CDS Primer A	AAGCAGTGGTATCAACGCAGAGTAC(T)30V N	3'RACE
NUP	AAGCAGTGGTATCAACGCAGAGT	5'RACE/3'RACE
UPM-long	CTAATACGACTCACTATAGGGCAAGCAGTGGTATCAACGCAGAGT	5'RACE/3'RACE
UPM-short	CTAATACGACTCACTATAGGGC	5'RACE/3'RACE
C2-qF	ATATCAACATGAAAACTCTTTTTCTT	Full-length cloning
C2-qR	TTAAGTTTTGGAAATAATTCAGTTTAA	Full-length cloning
C2-qF-1	ATGTCAACATGAAAACTCTTTTTCTTC	PCR
C2-qR-1	TTAAGTTTTGGAAATAATCCAGTTTAAA	PCR
C2-E-F1	<u>GGAATTC</u> ATGTCAACATGAAAACTCTTTTTTC	PCR
C2-X-R1	CCG <u>CTCGAGT</u> TAAGTTTTGGAAATAATCCAGT	PCR
T7 promoter primer	TAATACGACTCACTATAGGG	PCR
T7 Terminator Primer	GCTAGTTATTGCTCAGCGG	PCR
M13F(-47)	CGCCAGGGTTTTCCAGTCACGAC	PCR
M13R(-48)	AGCGGATAACAATTCACACAGGA	PCR

#### 4.5 Sequence analysis

The COX II amino acid sequence was deduced using the ExPASy ProtParam tool. The theoretical isoelectric point (pI) and molecular weight (Mw) of the deduced proteins were also predicted with using this web Tool. A multiple alignment analysis of the amino acid sequences was carried out using DNAMAN8.0 software. The secondary structure prediction was performed with Prabi-Gerland. Conserved domains were detected using the Conserved Domains Search tool. Transmembrane regions were predicted using the TMHMM server. Phylogenetic analyses were performed using MEGA 5.1 software with the neighbor-joining method, followed by phylogeny test options of 1000 bootstrap replicates.

#### 4.6 Vector construction and Expression at small scale

The COX II ORF was amplified with specific primer C2-E-F1 and C2-X-R1 (Table 1) containing *EcoRI* and *XhoI* restriction enzyme sites (underlined). The amplicons were purified, ligated and sequenced under the same conditions described above. The plasmid of sequenced clones were extracted from *E. coli* DH5 $\alpha$  and digested by restriction endonuclease *EcoRI* and *XhoI*. The digested COX II ORF was cloned into *EcoRI* and *XhoI* site pre-digestion of pET-32a plasmid using T4 DNA ligase and transformed into *E. coli* Transetta (DE3). The positive recombinant clones were further verified by digestion and sequencing. The recombinant proteins containing Trx/6-His/S-tag/ at N-terminus for purification.

For fusion protein expression, *E. coli* strains containing plasmids pET-32a-COX II were inoculated to 5 mL of Luria-Bertani (LB) medium including 100  $\mu$ g•mL Ampicillin(AMP). Cells were cultured overnight at 37°C with shaking at 200 rpm. 50  $\mu$ L cell suspension was inoculated to 5 mL of LB medium. when cell growth reached the exponential phase (OD<sub>600</sub>:0.5-0.7), Then inducing with 1 mM IPTG at 16°C, 25°C, 37°C with shaking at 200 rpm for 24 h, Cell pellets were harvested by centrifuged and sonicated for 5 min. After centrifugation for 20 min at 12,000 $\times$ g at 4 °C, the soluble and insoluble fractions were denatured and then submitted to a 12 % SDS-PAGE to determine the yield and solubility of expressed protein.

Different concentrations of IPTG (0.5mM, 1.0mM, 1.5mM, 2.0mM,) were investigated to determine the effect of IPTG on solubilization of COX II protein under the same conditions described above. Meanwhile, the survey of tested time (6 h, 12 h, 24 h, 36 h, 48 h, 60 h) was conducted to look into its effect on the solubility of COX II protein under 16°C, 1mM IPTG 200rpm, and soluble protein content were analyzed on a 12 % SDS-PAGE gel.

#### 4.7 Scale-up expression, Purification and Western Blot Analysis

According to the small-scale expression cultures exhibited the optimal amount of soluble protein, recombinant *E. coli* was induced in 1.8 L LB medium in the presence of 1 mM IPTG at 18°C under 24 h, 200 rpm, Bacterial cells were harvested by centrifugation and resuspended in 1 mL of 25 mM PBS buffer (pH 7.4) per 100 mg wet weight of cells, and then disrupted by sonication. Supernatant was separated from cell debris by centrifugation (12,000×g, 30 min, 4 °C) and clarified by passing them through a 0.45 µm filter before being applied to a Ni<sup>2+</sup>-NTA agarose gel column (TransGen, Beijing, China). The column was previously equilibrated with 10 volumes of PBS buffer to blance at a flow rate of 2mL/min according to the instruction manual. The column was washed with 6 volumes of wash buffer (10 mM PBS buffer, pH 7.4, 10 mM imidazole) after the sample was drained. The bound proteins were eluted from the affinity resin with 3 volumes of elute buffer (balance buffer containing a linear gradient of 50-400 mM imidazole), fractions were collected and analyzed on a 12 % SDS-PAGE gel.

Purified protein was verified via WB analysis with Horseradish peroxidase (HRP)-labeled Anti-His Tag Mouse Monoclonal Antibody and detected with a diaminobenzidine kit according to the instructions. The recombinant fusion COX II protein was dialyzed against PBS buffer/CaCl<sub>2</sub> (10 mM/L mM, pH 7.4) and then incubated overnight at room temperature with enterokinase (Solarbo, Beijing, China) to generate tag-free protein. The protein concentration was determined using the Bradford method [52].

#### 4.8 Assay of Enzymatic Activity

Cytc (Sigma, USA), was mainly the oxidized status, which can be prepared utilizing sodium ascorbate (solarbio, Beijing, China), 5µL of purified enzyme was added into 195µL of sample test buffer (16 mM Na<sub>2</sub>HPO<sub>4</sub>, 276 mM Na<sub>2</sub>HPO<sub>4</sub>, pH 5.8). The activity of protein was demonstrated by monitoring the oxidation process of the reduced cytochrome c (Cyt c), the UV spectrophotometer (Hitachi-3310, Japan) was used to characterize the reaction. A total of four treatment groups as follows (Table 2).

Furthermore, absorption peaks change of the purified COX II combination with AITC was detected according to the infrared spectrometer(Nicolet Avatar 330, USA). Through the observation of three different treatment of the peak pattern(Table 3), to determine whether the AITC and purified COX II have a combination.

**Table 2.** Assay of purified COX II Activity

grops	experimental treatments(200µL)
1	reduced Cyt c
2	reduced Cyt c+purified COX II
3	reduced Cyt c+purified COX II +AITC
4	reduced Cyt c+AITC

**Table 3.** Binding assay of AITC and purified COX II

grops	experimental treatments(200µL)
1	1µL AITC+199µL buffer
2	2µL purified COX II +198µL buffer
3	1µL AITC +2µL purified COX II +197µL buffer

#### 4.9 Homology modeling and molecular docking

With cytochrome C oxidase from bovine heart (PDB ID:1V54, PDB ID:1OCC) as a template, the three-dimensional structure of the COX II was constructed by Discovery Studio (DS) (Accelrys, USA) software homology modeling module, and then using the homologous protein method to search for the active pocket of the COX II, the Vina 1.1.2 Autodock software was used to carry out molecular docking study.

## 5. Conclusions

In summary, we have successfully cloned the COX II gene from the *Sitophilus zeamais*, and expressed the COX II fused with Trx/His/S-tags in the *E.coli* cells. In addition, the fusion proteins are purified and evaluated its activities towards Cyt c and AITC. Meanwhile, combining with molecular docking experimental was conducted. The results indicated that recombinant COX II was functional and might be one of the sites of action of AITC. The results

also provided that basis information for mechanism of AITC against adult *Sitophilus zeamais*.

**Acknowledgments:** The work was supported jointly by the National Natural Sciences Foundation of China (No.31101457) and the Fundamental Research Funds of Northwest Agriculture and Forestry University (No.2452015014).

**Author Contributions:** Changliang Hou and Hua Wu conceived and designed the experiments; Changliang Hou, Jingbo Wang and Jiayu Liu performed the experiments; Changliang Hou, Hua Wu, Zhiqing Ma and Juntao Feng analyzed the data; Xing Zhang contributed reagents/materials/analysis tools; Changliang Hou and Hua Wu wrote the paper.

**Conflicts of Interest:** The authors declare no conflict of interest.

#### Abbreviations:

COX II	Cytochrome c oxidase subunit II
Cco	Cytochrome c oxidase
ORF	open reading frame
WB	Western Blotting
AITC	allyl isothiocyanate
ROS	Reactive oxygen species
Mw	molecular weight
IPTG	isopropyl $\beta$ -D-thiogalactopyranoside

#### References

- [1] Howe, R.W. Losses caused by insects and mites in stored foods and feeding stuffs. *Nutrition Abstracts and Review*. **1965**, 35-285.
- [2] Danho, M.; Gaspar, C.; Haubruge, E. The impact of grain quantity on the biology of *Sitophilus zeamais*, *Motschulsky (Coleoptera: Curculionidae)*: oviposition, distribution of eggs, adult emergence, body weight and sex ratio. *Journal of Stored Products Research*. **2002**, 38, 259-266.
- [3] Jagadeesan, R.; Collins, P.J.; Darglish, G.J.; Ebert, P. R.; Schlipalius, D.I. Phosphine Resistance in the Rust Red Flour Beetle, *Tribolium castaneum* (Coleoptera: Tenebrionidae): Inheritance, Gene Interactions and Fitness Costs. *Plos One*. **2012**, 7, 347-350.
- [4] Price, N.R. The mode of action of fumigants. *Journal of Stored Products Research*. **1985**, 21, 157-164.
- [5] Small, G.J. A comparison between the impact of sulfuryl fluoride and methyl bromide fumigations on stored-product insect populations in UK flour mills. *Journal of Stored Products Research*. **2007**, 43, 410-416.
- [6] Athanassiou, C.G.; Phillips, T.W.; Aikins, M.J.; Hasan, M.M.; Throne, J.E. Effectiveness of sulfuryl fluoride for control of different life stages of stored-product psocids (Psocoptera). *Journal of Economic Entomology*, **2012**, 105, 282-287.
- [7] Zhi, L.L.; Sha, S.C.; Guo, H.J. Toxicity of *Schizonepeta multifida*, essential oil and its constituent compounds towards two grain storage insects. *Journal of the Science of Food & Agriculture*. **2011**, 91, 905-909.
- [8] Jembere, B.; Obeng-Ofori, D.; Hassanali, A.; Nyamasyo, G.N.N. Products derived from the leaves of *Ocimum kilimandscharicum* (Labiatae) as post-harvest grain protectants against the infestation of three major stored product insect pests *Bulletin of Entomological Research*. **1995**, 85, 361-367.
- [9] Okonkwo, E.U.; Okoye, W.I. The efficacy of four seed powders and the essential oils as protectants of cowpea and maize grain against infestation by *Callosobruchus maculatus* (Fabricius) (Coleoptera: Bruchidae) and *Sitophilus zeamais* (Motschulsky) (Coleoptera: Curculionidae) in Nigeria *International Journal of Pest Management*. **1996**, 42, 143-146.
- [10] Wu, H.; Zhang, G.A.; Zeng, S.; Lin, K.C. Extraction of allyl isothiocyanate from horseradish (*Armoracia rusticana*) and its fumigant insecticidal activity on four stored-product pests of paddy. *Pest Management Science*. **2009**, 65, 1003-1008.
- [11] Wu, H. Research on synthesis and properties of isothiocyanates and their biological activity against the harmful pests (Ph.D. dissertation), *HuaZhong Agricultural University*, **2010**, 23-25.
- [12] Wu, H.; Liu, X.R.; Yu, D.D.; Zhang, X.; Feng, J.T. Effect of allyl isothiocyanate on ultra-structure and the activities of four enzymes in adult *Sitophilus zeamais*. *Pesticide Biochemistry and Physiology*. **2014**, 109, 12-17.
- [13] Zhang, C.; Wu, H.; Zhao, Y.; Ma, Z.Q.; Zhang, X. Comparative studies on mitochondrial electron transport chain complexes of *Sitophilus zeamais* treated with allyl isothiocyanate and calcium phosphide. *Pesticide Biochemistry and Physiology*. **2016**, 126, 70-75.
- [14] Mansour, E.E.; Mi, F.; Zhang, G.; Xie, J.; Wang, Y.; Kargbo, A. Effect of allyl isothiocyanate on *Sitophilus oryzae*, *Tribolium confusum* and *Plodia interpunctella*: Toxicity and effect on insect mitochondria. *Crop Protection*. **2012**, 33, 40-51.
- [15] Sousa, F.L.; Alves, R.J.; Ribeiro, M.A.; Ma, J.; Gennis, R.B. The superfamily of heme-copper oxygen reductases: Types and

- evolutionary considerations. *Biochimica Et Biophysica Acta*, **2012**, 1817, 629-637.
- [16] Yoshikawa, S.; Muramoto, K.; Shinzawaitoh, K. Proton-pumping mechanism of cytochrome C oxidase. *Annual Review of Biophysics*. **2011**, 40, 205-223.
- [17] Renger, G.; Ludwig, B. Mechanism of Photosynthetic Production and Respiratory Reduction of Molecular Dioxide: A Biophysical and Biochemical Comparison. *Springer Netherlands*, **2011**. 337-394.
- [18] Kyoko, S.I.; Hiroshi, A.; Muramoto, K.; Terada, H.; Kurauchi, T.; Tadehara, Y.; Yamasaki, A.; Sugimura, T.; Kurono, S.; Tsujimoto, K.; Mizushima, T.; Yamashita, E.; Tsukihara, T.; Yoshikawa, S. Structures and physiological roles of 13 integral lipids of bovine heart cytochrome c oxidase. *Embo Journal*, **2007**, 26, 1713-25.
- [19] Poynter, D. Structural studies on bovine heart cytochrome c oxidase. *Biochimica Et Biophysica Acta*, **1985**, 1817, 579-89.
- [20] Kadenbach, B.; Jaraus, J.; Hartmann, R.; Merle, P. Separation of mammalian cytochrome c oxidase into 13 polypeptides by a sodium dodecyl sulfate-gel electrophoretic procedure. *Analytical Biochemistry*, **1983**, 129, 517-521.
- [21] Dash, B.P.; Alles, M.; Bundschuh, F.A.; Richter, O.M.H.; Ludwig, B. Protein chaperones mediating copper insertion into the Cu site of the aa<sub>3</sub>-type cytochrome c oxidase of *Paracoccus denitrificans*. *Biochimica et Biophysica Acta-Bioenergetics*, **2014**, 1847, 202-211.
- [22] Vygodina, T.V.; Kirichenko, A.; Konstantinov, A.A. Cation binding site of cytochrome c oxidase: progress report. *Biochimica Et Biophysica Acta*. **2014**, 1837, 1188-1195.
- [23] Siegbahn, P.E.M.; Blomberg, M.R.A. Mutations in the d-channel of cytochrome c oxidase causes leakage of the proton pump. *FEBS Letters*. **2014**, 588, 545-548.
- [24] Musatov, A.; Robinson, N.C. Bound cardiolipin is essential for cytochrome c oxidase proton translocation. *Biochimie*. **2014**, 105, 159-164.
- [25] Mi, L.; Pasqua, A.J.D.; Chung, F.L. Proteins as binding targets of isothiocyanates in cancer prevention. *Carcinogenesis*, **2011**, 32, 1405-1413.
- [26] Kassie, F.; Knasmüller, S. Genotoxic effects of allyl isothiocyanate (AITC) and phenethyl isothiocyanate (PEITC). *Chemico-biological interactions*, **2000**, 127, 163-180.
- [27] Mi, L.; Hood, B.L.; Stewart, N.A.; Xiao, Z.; Govind, S.; Wang, X. Identification of Potential Protein Targets of Isothiocyanates by Proteomics. *Chemical Research in Toxicology*, **2011**, 24, 1735-43.
- [28] Li, T.; Zhang, Y. Mitochondria are the primary target in isothiocyanate-induced apoptosis in human bladder cancer cells. *Molecular Cancer Therapeutics*, **2005**, 4, 1250-1259.
- [29] Hahm, E.R.; Singh, S.V. Sulforaphane inhibits constitutive and interleukin-6-induced activation of signal transducer and activator of transcription 3 in prostate cancer cells. *Cancer Prevention Research*, **2010**, 3, 484-94.
- [30] Hollenberg, P.F.; Kent, U.M.; Bumpus, N.N. Mechanism-based inactivation of human cytochromes p450s: experimental characterization, reactive intermediates, and clinical implications. *Chem.res.toxicol*, **2008**, 21, 189-205.
- [31] Mi, L.; Gan, N.; Chung, F.L. Isothiocyanates inhibit proteasome activity and proliferation of multiple myeloma cells. *Carcinogenesis*, **2011**, 32, 216-223.
- [32] Mukherjee, S.; Dey, S.; Bhattacharya, R.K.; Roy, M. Isothiocyanates sensitize the effect of chemotherapeutic drugs via modulation of protein kinase C and telomerase in cervical cancer cells. *Molecular & Cellular Biochemistry*, **2009**, 330, 9-22.
- [33] Li, T.; Zhang, Y. Mitochondria are the primary target in isothiocyanate-induced apoptosis in human bladder cancer cells. *Molecular Cancer Therapeutics*, **2005**, 4, 1250-1259.
- [34] Santos, J.C.; Faroni, L.R.A.; Sousa, A.H.; Guedes, R.N.C. Fumigant toxicity of allyl isothiocyanate to populations of the red flour beetle *Tribolium castaneum*. *Journal of Stored Products Research*, **2011**, 47, 238-243.
- [35] Hosler, J.P.; Fergusonmiller, S.; Mills, D.A. Energy Transduction: Proton Transfer Through the Respiratory Complexes. *Annual Review of Biochemistry*. **2006**, 75, 165-187.
- [36] Belevich, I.; Verkhovsky, M.I. Molecular mechanism of proton translocation by cytochrome c oxidase. *Antioxidants & Redox Signaling*. **2008**, 10, 1-29.
- [37] Kaila, V.R.; Verkhovsky, M.I.; Wikström, M. Proton-Coupled Electron Transfer in Cytochrome Oxidase. *Chemical Reviews*. **2010**, 110, 7062-7081.
- [38] Wei, S.J.; Min, S.; Chen, X.X.; Sharkey, M.J.; Achterberg, C.V.; Ye, G.Y. New views on strand asymmetry in insect mitochondrial genomes. *Plos One*. **2009**, 5, 490-491.
- [39] Martínez-Alonso, M.; García-Fruitós, E.; Villaverde, A. Yield, solubility and conformational quality of soluble proteins are not simultaneously favored in recombinant *Escherichia coli*. *Biotechnology & Bioengineering*. **2008**, 101, 1353-1358.

- [40] Vera, A.; González-Montalbán, N.; Aris, A.; Villaverde, A. The conformational quality of insoluble recombinant proteins is enhanced at low growth temperatures. *Biotechnology & Bioengineering*. **2007**, *96*, 1101-1106.
- [41] Pope, W.H.; Haase-Pettingell, C.; King, J. Protein folding failure sets high-temperature limit on growth of phage P22 in *Salmonella enterica* serovar Typhimurium. *Applied & Environmental Microbiology*. **2004**, *70*, 4840-4847.
- [42] Scharnagl, C.; Reif, M.; Friedrich, J. Stability of proteins: Temperature, pressure and the role of the solvent. *Biochimica Et Biophysica Acta*. **2005**, *1749*, 187-213.
- [43] Yang, X.; Zhang, Y.; Effect of temperature and sorbitol in improving the solubility of carboxylesterases protein CpCE-1 from *Cydia pomonella*, and biochemical characterization. *Applied Microbiology & Biotechnology*. **2013**, *97*, 10423-10433.
- [44] Pinakoulaki, E.; Pfitzner, U.; Ludwig, B.; Varotsis, C. Direct Detection of Fe(IV)=O Intermediates in the Cytochrome aa3 Oxidase from *Paracoccus denitrificans*/H<sub>2</sub>O<sub>2</sub> Reaction. *Journal of Biological Chemistry*. **2003**, *278*, 18761-18766.
- [45] Finel, M.; Wikström, M. Studies on the role of the oligomeric state and subunit III of cytochrome oxidase in proton translocation. *Biochimica Et Biophysica Acta*. **1986**, *851*, 99-108.
- [46] Wilson, K.S.; Prochaska, L.J. Phospholipid vesicles containing bovine heart mitochondrial cytochrome c, oxidase and subunit III-deficient enzyme: Analysis of respiratory control and proton translocating activities. *Archives of Biochemistry & Biophysics*. **1990**, *282*, 413-420.
- [47] Lincoln, A.J.; Donat, N.; Palmer, G.; Prochaska, L.J. Site-specific antibodies against hydrophilic domains of subunit III of bovine heart cytochrome c, oxidase affect enzyme function. *Archives of Biochemistry & Biophysics*. **2003**, *416*, 81-91.
- [48] Bratton, M.R.; Pressler, M.A.; Hosler, J.P. Suicide inactivation of cytochrome c oxidase. Catalytic turnover absence subunit III alters active site. *Biochemistry*. **2000**, *38*, 16236-16245.
- [49] Varanasi, L.; Hosler, J.P. Subunit III-depleted cytochrome c, oxidase provides insight into the process of proton uptake by proteins. *Biochimica Et Biophysica Acta*, **2012**, *1817*, 545-551.
- [50] Li, Y.Q.; Liu, J.W.; Lu, M.; Ma, Z.Q.; Cai, C.L.; Wang, Y.H. Bacterial Expression and Kinetic Analysis of Carboxylesterase 001D from *Helicoverpa armigera*. *International Journal of Molecular Sciences*. **2016**, *17*.
- [51] Zhu, C.; Chen, X.; Guo, J.; Miao, G.; Feng, J.; Zhang, X. Cloning and expression analysis of 1-deoxy-D-xylulose 5-phosphate reductoisomerase gene (DXR) in *Tripterygiun wilfordii*. *Agric. Biotechnol.* **2014**, *22*, 298-308.
- [52] Bradford, M.M. A rapid and sensitive method for the quantitation of microgram quantities of protein utilizing the principle of protein-dye binding. *Anal. Biochem.* **1976**, *72*, 248-254.



© 2016 by the authors; licensee *Preprints*, Basel, Switzerland. This article is an open access article distributed under the terms and conditions of the Creative Commons by Attribution (CC-BY) license (<http://creativecommons.org/licenses/by/4.0/>).